

Self-supervised training for blind multi-frame video denoising

Valéry Dewil, Jérémy Anger, Axel Davy, Thibaud Ehret, Pablo Arias, and
Gabriele Facciolo

CMLA, ENS Cachan, CNRS
Université Paris-Saclay, 94235 Cachan, France

Abstract. We propose a self-supervised approach for training multi-frame video denoising networks. These networks predict frame t from a window of frames around t . Our self-supervised approach benefits from the video temporal consistency by penalizing a loss between the predicted frame t and a neighboring target frame, which are aligned using an optical flow. We use the proposed strategy for online internal learning, where a pre-trained network is fine-tuned to denoise a new unknown noise type from a single video. After a few frames, the proposed fine-tuning reaches and sometimes surpasses the performance of a state-of-the-art network trained with supervision. In addition, for a wide range of noise types, it can be applied blindly without knowing the noise distribution. We demonstrate this by showing results on blind denoising of different synthetic and realistic noises.

Keywords: video denoising, blind denoising, neural networks, self-supervised training, online training

1 Introduction

Denoising has been a fundamental problem of image and video processing since the early days of these disciplines. It continues to be an active research problem thanks to the continuous need for reduced sensor size and the desire of imaging in increasingly challenging conditions (such as low light and short exposure times).

The current state-of-the-art in image and video denoising is dominated by convolutional neural networks [71,56,12,42,50,68,18,60]. In addition to their superior performance, CNNs offer a greater flexibility as they can be trained to denoise potentially any type of noise [12,27,66,29,10]. In contrast, traditional model-based approaches typically require a tractable model of the noise, and require specific algorithms for each noise (e.g. [38,25,43,54,16,5,72]). This flexibility however, comes at a price, as it has been observed that CNNs are very sensitive to miss-matches between the noise distributions at training and testing [49]. This has fueled the interest in training CNNs for realistic noise, with the publication of several datasets and benchmarks [48,49,12,1,7], as well as methods for removing realistic noise [27,6,50,32]. All this research focuses almost exclusively on still image denoising.



Fig. 1: Denoising results on Poisson noise ($p = 8$), Box noise ($\sigma = 40, 3 \times 3$) and demosaicked Poisson noise ($p = 4$). From left to right: noisy frame, FastDVDnet (supervised for each noise type), F2F (self-supervised), proposed offline method (self-supervised).

Producing realistic noisy-clean datasets for supervised training is a challenging task. Some works contaminate clean images with synthesized realistic noise [27,6], but the results depend on the fit between the synthetic and real noises. Generative Adversarial Networks have been proposed to learn to sample from a unknown noise distribution [13]. In the case of still images it is possible to acquire pairs of images of exactly the same scene, either altering the exposure time so that one is approximately clean [49,12,11], or by taking a second noisy shot with an independent noise realization as proposed by *noise-to-noise* [39]. In practice it is cumbersome to acquire such pairs and prone to dataset biases as the scenes need to be static. In video the situation is even worse as it would require two independent acquisitions of the exact same action.

A more ambitious goal is that of *self-supervised* training, where the network learns exclusively from noisy images/videos that are used as input as well as target in the loss. To prevent the network from learning the identity function some methods [45,58] resort to using Stein’s unbiased risk estimator, however this requires white Gaussian noise and MSE loss. *Blind-spot* networks [35,4,36,37] exploit instead the spatial regularity of images by training the network to predict the center of the receptive field from its surrounding. The performance of these networks is however limited by this spatial regularity hypothesis.

In videos, the strong temporal redundancy has been exploited for self-supervised learning in many applications, such as tracking [64,65], object segmentation [9] and action classification [57,67,24,20,47]. However, the treatment of real noise in videos has received much less attention. Patch-based approaches have been proposed for handling correlated noise in compressed videos [41] and infrared

videos [43]. In [46,44,15] CNNs are trained by synthesizing signal dependent noise. In [11] an image denoising network is trained on low-light static sequences using a long exposure image as ground truth. A temporal consistency loss is added to better generalize to dynamic scenes. Recently, Ehret et al. [22] proposed a method to fine-tune an image denoising network to an unknown noise type from a single noisy video. We will refer to this framework as *frame-to-frame* (F2F) in reference to the *noise-to-noise* framework. The fine-tuning is based on a noise-to-noise loss [39] that penalizes the motion compensated error between the predicted frame and the previous noisy frame as *target*. The fine-tuned network achieved (and even surpassed) the performance of the same network trained with supervision for that specific noise. An important limitation of F2F is that its single-frame denoising network leads to sub-optimal video denoising results and lacks of temporal consistency.

Contributions. In this work we extend the F2F approach of [22] to video denoising networks that take as input a *stack* of several neighboring frames as input. We call it Multi-frame-to-frame (MF2F). A problem occurs if the target frame in the loss is part of the input stack of frames, as the network learns to output the target frame (warped if needed). By evaluating different options for the input stack using the FastDVDnet video denoising network [60], which takes five frames as input, we show that the straightforward extension (taking the target frame outside of the input stack) is not optimal. Best performance is achieved by modifying the input stack to exclude target frame $t - 1$, similarly to blind-spot networks [34,4].

We also show that optical flow errors are more problematic with video denoising networks. The removal of alignment errors as done in [22] creates a training bias that leads to salient artifacts around motion discontinuities after fine-tuning. For addressing this problem we propose to use a secondary weak denoiser as target in the areas with large alignment errors. The weak denoiser is not fully fine-tuned so that it does not suffer from the same forgetting, and it can act as a memory that “teaches” the primary network how to handle the removed regions. As “teacher” network we use the same FastDVDnet pre-trained for AWGN, but we fine-tune only a variance map, which FastDVDnet takes as input. In this way we make sure that it does not suffer from forgetting. The teacher network by itself might produce poorer denoising results, but its output is only used as training target in a small fraction of the frame.

Starting from a network pre-trained for white additive Gaussian noise, we demonstrate the effectiveness of the proposed approach by fine-tuning the weights to different noise types (AWGN, Poisson, colored Gaussian and demosaicked Poisson) and levels. The network adapts to removing noise of unknown distribution using *a single noisy sequence*. We achieve results competitive to the same network trained with supervision on a large external dataset for that same noise (see Fig. 1). To the best of our knowledge, this is the first blind video denoising method achieving state-of-the-art results on a wide range of noise types.

In Section 2 we discuss previous self-supervised approaches for image and video restoration. The proposed method is described in Section 3, after which we present empirical results in Section 4. Concluding remarks are given in Section 5.

2 Self-supervised learning and data-driven learning

Suppose we want to predict y from x . In our case, x is a stack of noisy frames and y the clean version of the central frame of the stack, but the arguments in this section apply as well to other regression problems. In a supervised training setting we minimize the expected value of a loss penalizing the difference between the network output and the desired y :

$$\mathcal{R}^{\text{emp}}(\mathcal{F}) = \frac{1}{m} \sum_{i=1}^m \ell(\mathcal{F}(x_i), y_i) \approx \mathbb{E}_{x,y} \{\ell(\mathcal{F}(x), y)\}, \quad (1)$$

where the approximation holds if the number m of training samples is sufficiently large. The optimal estimator depends on the loss. For instance, for the MSE loss we have $\mathcal{F}^*(x) = \mathbb{E}\{y|x\}$ or for the L_1 loss we have the median of the posterior distribution $\mathcal{F}^*(x) = \text{median}\{y|x\}$ [30]. The network learns from the data to output estimators that depend on the posterior distribution $p(y|x)$, which in turn depends on the prior $p(y)$ and the data likelihood $p(x|y)$ (the noise distribution in a denoising setting). These are examples of data-driven estimators. This is stark contrast to traditional model-based approaches that used hand-crafted priors and noise models. Such approaches are often formulated as an energy minimization problem:

$$\hat{y}(x) = \arg \min_{\hat{y}} \mathcal{D}(\hat{y}, x) + \mathcal{R}(\hat{y}), \quad (2)$$

where \mathcal{D} is a data attachment term and \mathcal{R} a regularization term. The resulting estimator only depends on the chosen energy and the observed x .

Some unsupervised learning methods for low-level vision tasks such as motion and depth estimation proposed use losses inspired by traditional model-based approaches [62,52], with a data term measuring the consistency between the network output and the input data (for instance photo-consistency) and regularization terms that impose smoothness on $\mathcal{F}(x)$

$$\ell(\mathcal{F}(x), x) = \mathcal{D}(\mathcal{F}(x), x) + \mathcal{R}(\mathcal{F}(x)). \quad (3)$$

However, the optimal estimators for such losses are not data driven as defined above. As the loss depends only on the input x and $\mathcal{F}(x)$, the minimization of $\mathbb{E}\{\ell(\mathcal{F}(x), x)\}$ can be done for each input x independently, i.e. $\mathcal{F}^*(x) = \arg \min_{\hat{y}} \mathcal{D}(\hat{y}, x) + \mathcal{R}(\hat{y})$. This is essentially the same situation than for model-based approaches: given x , the optimal estimator only depends on the hand-crafted loss, while it is independent on the data distribution. The difference is that instead of computing $\hat{y}(x)$ via an optimization algorithm, a network trained to predict the minimizer. We can generalize this as the following:

Observation 1. *Suppose (x, y) distributed according to $p(x, y)$. An estimator $\hat{y}(x) = \mathcal{F}^*(x)$ minimizing the expected value of a loss $\mathbb{E}\{\ell(\mathcal{F}(x), x)\}$ that depends only on x and $\mathcal{F}(x)$ is independent from the data distribution $p(x, y)$.*

Interestingly, *it is possible* to learn data-driven Bayesian estimators such as the MMSE via the minimization of an energy that only depends on the noisy input [26,8]. This requires however regularization terms that depend on the noise $p(x|y)$ and the data distribution $p(y)$, which are unknown in most practical cases.

For image denoising, self-supervised approaches minimize some variant of the self reconstruction risk, which for the MSE loss is given by:

$$\mathcal{R}(\mathcal{F}) = \sum_i \|\mathcal{F}(x_i) - x_i\|^2, \quad (4)$$

This risk is minimized by the identity function $\mathcal{F}^*(x) = x$ and two main approaches have been proposed to escape this trivial solution.

In [45,58] the authors use Stein’s unbiased risk estimator (SURE) [59] to estimate the supervised MSE risk. This amounts to adding a term to the risk, which penalizes the divergence of the estimator \mathcal{F} with respect to the input data $\text{div}_x \mathcal{F}(x)$.¹ SURE-like estimators of the MSE risk have been derived for other inverse problems [45], and for other noise distributions [51,19]. Unfortunately, they only work for the MSE risk and require the noise distribution to be known.

The other approach to avoid the identity as solution of (4) is to remove it from the set of solutions by restricting the network architecture. Denoising autoencoders [63] use a bottleneck forcing the network to filter out information. *Blind-spot* networks [34,4] are not allowed to use the input pixel at j for computing the output pixel j (a blind spot at the center of the receptive field).

For a blind-spot network, with the MSE loss, self-supervised training is asymptotically equivalent to supervised training if the noise is spatially invariant [4]. However, the blind spot has an significant penalty on the performance, as the noisy value of a pixel is a valuable piece of information for denoising it. Some works re-introduce the blind spot in a second Bayesian estimation step [37,36]. Although this greatly improves the denoising performance, it requires knowing the noise distribution, plus it does not apply to spatially correlated noise.

In summary, no current approach for self-supervised learning of single image denoising is comparable to supervised training for a wide range of noise types. The situation in a video more favorable due to the strong temporal correlation.

Our work is inspired by methods that used self-supervised training for fine-tuning a network to a single video for video segmentation, [9], denoising [22], and stereo [73,62]. In [22] the network takes a single frame as input and is trained to predict the previous (or next) frame. This training can be done frame-by-frame in an fashion. The main limitation of these approaches is that the networks take as input a single frame which gives much worse results compared to multi-frame video denoising networks.

¹ SURE’s divergence term can be interpreted as a sort of regularization, but is not a function of an individual network’s output $\mathcal{F}(x)$, so Observation 1 does not apply.

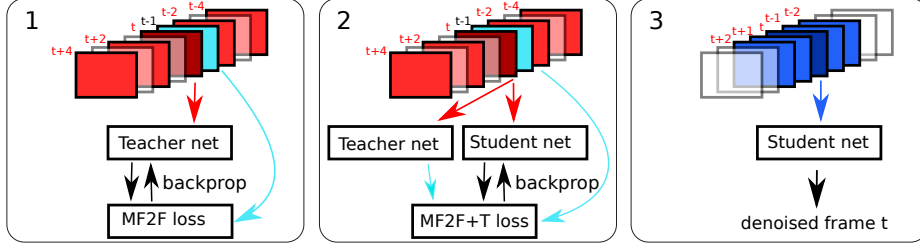


Fig. 2: Overview of the proposed multiframe-to-frame blind fine-tuning for a video denoising network taking as input a stack of frames. The algorithm applies three steps for each frame t . The noise parameter of the “teacher” network is fine-tuned (step 1) with the MF2F loss (6), which compares the output of the network with the previous frame $t - 1$ (frames are aligned to compensate for motion). A similar MF2F+T loss (9) is used to fine-tune the “student” network (step 2), except that at locations where alignment errors are detected the output of a “teacher” network is used as target. During fine-tuning we use a dilated input stack (in red) so that the target frame is hidden from the network. At inference time (step 3) we use the natural stack (in blue).

Some works take self-supervision to the extreme, and train the network using only the input image to be restored [40,3,70]. Our work is related to these approaches as we fine-tune a pre-trained video denoising network using a single noisy video.

3 Self-supervised Video Denoising

We consider a video f with frames f_t , which is a noisy version of a video u . The distribution of the noise is unknown. We assume that the noise at each frame is independent, and that is median preserving in the noise-to-noise sense [39,22].

Our self-supervised loss for video denoising extends the F2F loss introduced in [22], which penalizes the output of the network at frame t with a target frame at $t - 1$ (the *target* frame). The authors of [22] consider a denoising network \mathcal{F}_θ which takes a single image as input, and train it via the following loss:

$$\ell_1^{\text{F2F}}(\mathcal{F}_\theta(f_t), f_{t-1}) = \|\kappa_t \circ (W_{t,t-1}\mathcal{F}_\theta(f_t) - f_{t-1})\|_1. \quad (5)$$

Here \circ denotes the element-wise product, $W_{t,t-1}$ the warping operator from the current frame t to the target frame $t - 1$, and κ_t is an occlusion mask removing miss-matches from the loss. The warping operator can be computed using an optical flow algorithm or a global transformation estimated between both frames (such as a homography as in [21]).

In [22] the temporal consistency of the video is used to train the network but the network itself takes as input a single image. Better results can be obtained by network architectures that take into account temporal information. This can be

done with frame recurrent networks [14] or by providing multiple frames as the input of the network [68,18,60]. We focus on the latter type of networks as they have produced state-of-the-art results in video denoising. In particular, we will adopt the recent FastDVDnet [60]², which consists of two cascaded U-nets [53], each of which takes as input three frames without alignment. The first U-net accesses the input noisy frames and is applied three times to produce an initial estimate of frames $t-1$, t and $t+1$. These are fed into the second network which predicts the central frame. Thus, the overall architecture takes five frames as input and is trained end-to-end. Additionally, a variance map is concatenated as an additional input channel. This architecture has the advantage of not explicitly including a motion estimation stage. Due to their large receptive fields, U-net blocks were shown to be able to cope implicitly with motion [28].

We denote the input stack of frames as $\mathcal{S}_t = [f_{t-n}, \dots, f_t, \dots, f_{t+n}]$. The t^{th} denoised frame is produced as $\hat{u}_t = \mathcal{F}_\theta(\mathcal{S}_t)$.

3.1 A Loss for Self-supervised Video Denoising

The F2F loss (5) cannot be directly applied to $\mathcal{F}_\theta(\mathcal{S}_t)$, as the loss can be minimized by simply learning to warp f_{t-1} (which is in the input stack) to $W_{t,t-1}^{-1}f_{t-1}$, i.e. by aligning the noisy frame f_{t-1} to f_t without removing the noise. In fact, as argued in Observation 1 in §2, a network cannot learn a data-driven estimator if the loss is a function of the input \mathcal{S}_t and the network output $\mathcal{F}_\theta(\mathcal{S}_t)$. Thus we will adopt a solution similar to that of blind spot networks: remove the target from the input.

Training input stack. There are many ways of selecting the input stack and the target frame so that they do not overlap. For example, we can consider keeping the same input stack with frames $[f_{t-2}, \dots, f_{t+2}]$, and using $t \pm 3$ as target frames. Or conversely, we can keep the target frame as $t-1$ and introduce a “blind-spot” in the input stack: $[f_{t-3}, f_{t-2}, f_t, f_{t+1}, f_{t+2}]$. After evaluating all reasonable possibilities we found that: (1) The target frame has to be as close as possible to the denoised frame. Otherwise, the quality of the alignment degrades, negatively impacting the fine-tuning. (2) The best results were obtained using the stack $[f_{t-4}, f_{t-2}, f_t, f_{t+2}, f_{t+4}]$, which constitutes an even dilation of the natural stack. We believe that the reason for this is that FastDVDnet processes the input frames by sliding in time a U-net that takes 3 frames at a time. With a stack that alters the motion unevenly (by removing for example only the target frame) this U-net would see different motion patterns at each of the three positions it is used. A comparison of the different stacks is done in §4.

Fine-tuning loss. Denoting by \mathcal{S}'_t the dilated training stack, we then minimize the following *multi-frame to frame* (MF2F) loss:

$$\ell_1^{\text{MF2F}}(\mathcal{F}_\theta(\mathcal{S}'_t), f_{t-1}) = \|\kappa_t \circ (W_{t,t-1}\mathcal{F}_\theta(\mathcal{S}'_t) - f_{t-1})\|_1. \quad (6)$$

² The proposed fine-tuning can be applied to other multi-frame networks.



Fig. 3: Illustration of the forgetting effect: without proper care, the network unlearns how to handle moving objects (c). With the proposed mask and student-teacher mechanism, fast moving objects are correctly restored (d).

Given the optical flow $v_{t-1,t}$, the warping operator from frame $t-1$ to t is defined as

$$(W_{t,t-1}u_t)(x) = u_t(x + v_{t-1,t}(x)), \quad (7)$$

where bicubic interpolation is used to resample the image u_t .

Following [22], we compute the optical flow with the TV-L1 variational method [69,55], as it gives consistent results across noise types and intensities. Moreover, it is based on minimizing the photometric distance between pixels, which is precisely what we need for our loss.

The mask κ is zero for regions where an alignment error is likely, and one otherwise. Alignment errors are defined as the union of occlusions computed from the optical flow (similar to [22]) and regions with a large warping residue

$$r_{t,t-1} = g * \|W_{t,t-1}(g * f_t) - g * f_{t-1}\|_1, \quad (8)$$

where g is Gaussian filter of standard deviation $\sigma = 2$ used to obtain a rough estimate of the clean video. The warping residue is then thresholded with a robust adaptive threshold computed from the statistics of the warping residual. Details can be found in the supplementary material.

Forgetting and the teacher network. As will be shown in Section 4, with the proposed MF2F loss (6) we can attain state-of-the-art denoising performance for a wide range of noise types by fine-tuning the weights of FastDVDnet [60] originally trained for AWGN. In spite of this good performance, some results show a salient artifact: some fast moving objects become semi-transparent close to the motion boundary as shown in Fig. 3. This problem does not affect much the PSNR and is only sometimes noticeable while watching the video. However it may harm applications that require frame-by-frame analysis. Fig. 3 shows that removing the teacher on the occlusion mask leads to transparency artifacts, and that removing the occlusion mask and the teacher altogether results in even worse artifacts.

The cause for this artifact is the removal of some pixels from the loss with the mask κ_t . Fast moving objects cause large occluded and dis-occluded areas

where the warping is not well-defined. For these reasons, the boundaries around fast moving objects are systematically removed from the loss. Thus the network is never fine-tuned on such regions. As we update the weights of the network, it “unlearns” how to process these regions. This is similar to the phenomenon of *catastrophic forgetting* [33] observed when sequentially learning multiple tasks.

To alleviate the forgetting effect, we introduce a weak denoiser and use its output as target at motion boundaries. We call this weak denoiser the teacher as it “teaches” our network (the student) how to handle motion boundaries. We will denote the teacher and student networks with superindices “T” and “S”. Let \hat{u}_t^T be the output at frame t produced by the teacher network. Then, we propose to use the following loss function for the student network

$$\ell_1^{\text{MF2F+T}}(\mathcal{F}_\theta^S(\mathcal{S}'_t), f_{t-1}, \hat{u}_t^T) = \ell_1^{\text{MF2F}}(\mathcal{F}_\theta^S(\mathcal{S}'_t), f_{t-1}) + \|(1 - \kappa_t) \circ (\mathcal{F}_\theta(\mathcal{S}'_t) - \hat{u}_t^T)\|_1, \quad (9)$$

where the output of the teacher network is only used at the areas with alignment errors.

The teacher itself can be fine-tuned to some extent using (6), but care must be taken so that it does not suffer forgetting. In this work we considered as teacher the FastDVDnet network trained for AWGN, where the original weights have been frozen. Instead, we control the denoising strength by updating the variance map of the teacher by minimizing the original MF2F loss (6). While its denoising performance might be suboptimal when the noise is not AWGN, it will not forget how to handle motion boundaries as only the variance map is updated.

3.2 Fine-tuning and Inference

Similarly to [22], the proposed fine-tuning can be done online or offline. As illustrated in Fig. 2, the scheme processes the video applying three steps on very frame: (1) At frame t the input variance map of the teacher network is updated using (6). The teacher’s output \hat{u}_t^T is computed with the updated variance map and the natural stack. (2) The weights of the student network are updated using (9). (3) Finally, the denoised frame is computed with the updated student network evaluated on the natural stack.

To update both the teacher and the student networks, we perform a fixed number N of optimizer steps on the losses (6) and (9). A pseudo-code is given in the supplementary material. The online setting defines a time-varying sequence of teacher and student networks, and can therefore adapt to temporal changes in the distribution of the noise.

In the offline setting the video is considered as a dataset of frames, and the steps are applied to the whole video sequentially: we first train the teacher, then use its output to train the student, and then apply the student on the natural stack. During training, we form batches by randomly sampling stacks of frames from the video and update the network weights by performing one optimizer step per batch. This is repeated a fixed number of epochs.

Table 1: Average PSNR over all the sequences for a given dataset and type of noise. The best PSNR is in *italic*. The best blind method is in **bold**

		Noise blind methods							
Sequence		FDVDnet superv.	VBM3D	F2F	MF2F		Offline	MF2F	FDVDnet
					no teach.	teach.	no teach.	teach.	8 sigmas
Derf	Gauss. 20	36.97	36.21	33.70	37.19	37.23	<i>37.41</i>	37.20	36.88
	Gauss. 40	34.00	32.63	31.15	34.15	34.20	<i>34.24</i>	34.15	33.87
	Poiss. 1	<i>40.45</i>	38.99	36.56	40.28	40.38	40.44	40.43	40.10
	Poiss. 8	<i>35.30</i>	33.62	31.98	34.84	34.90	34.98	35.12	34.94
	Box 40 3	35.42	29.94	32.55	35.45	35.31	<i>35.58</i>	34.89	34.32
	Box 65 5	<i>34.78</i>	28.36	31.78	34.27	34.04	34.34	33.47	32.60
	Mosa. 4	<i>34.85</i>	33.16	32.61	34.66	34.60	34.77	34.60	34.25
NTIRE	Gauss. 20	37.49	36.55	31.62	37.22	37.41	37.49	<i>37.51</i>	37.40
	Gauss. 40	<i>34.27</i>	32.74	29.10	34.13	34.19	34.24	<i>34.27</i>	34.21
	Poiss. 1	<i>40.63</i>	39.32	33.54	39.89	40.22	40.17	40.40	40.28
	Poiss. 8	<i>35.72</i>	32.16	29.92	34.94	35.16	35.02	35.46	35.44
	Box 40 3	<i>37.28</i>	30.19	31.27	36.60	36.40	36.79	35.82	34.92
	Box 65 5	<i>36.81</i>	28.53	30.75	35.65	35.29	35.80	34.44	33.12
	Mosa. 4	<i>34.50</i>	32.31	31.59	33.92	34.04	33.96	34.09	33.89

We propose to use a different stack for training and testing. The network is trained with the dilated stack \mathcal{S}'_t , but testing is done with the natural stack \mathcal{S}_t . The frames in the natural stack are more temporally correlated and this helps improving the performance of the denoising.

4 Experiments

In this section we demonstrate the adaptability of the proposed blind video denoising method. We first describe the experimental setup and the considered algorithms, then we analyze the results and perform ablation studies to determine the impact of the different choices. Lastly we present some experiments obtained on videos with real noise of unknown statistics.

The starting point for all the fine-tuning experiments is the FastDVDnet network [60] trained for AWGN in which we fix the initial noise map to $\sigma = 25$. In all the experiments we use the same hyper-parameters for the fine-tuning: a learning rate of 10^{-5} and $N = 20$ iterations of the Adam optimizer per frame for the online training; the same learning rate is used for the offline training and 200 iterations of the Adam optimizer with mini-batches of 20 frames (no improvement was observed with more iterations). The parameters of the TV-L1 optical flow and the alignment error mask are also fixed for all experiments.

Experimental setup. The evaluation is performed on videos from two datasets. One is a set of seven Full HD sequences of 100 frames each extracted from the

Derfs Test Media collection³. The second, more challenging, dataset consists of ten sequences of 120 frames each extracted from the training dataset for the NTIRE 2020 Video Quality Mapping Challenge.⁴ Following [2] all the sequences have been downsampled by a factor two in each direction to ensure that they contain little to no noise.

In our experiments we consider four types of noise (1) AWGN noise, (2) scaled Poisson noise with scaling parameter p (the mean of the noisy pixel f_i is the clean pixel u_i , and the variance is pu_i), (3) correlated “box noise”, obtained by filtering AWGN with an $s \times s$ box filter and (4) demosaicked Poisson noise, obtained by mosaicking the image, adding scaled Poisson noise and then applying the demosaicking algorithm of [31]. For the first three types we consider two noise levels, indicated in the first columns of Table 1. The demosaicked Poisson noise simulates the correlation introduced by a demosaicking algorithm. We evaluate the average PSNR and SSIM for the given sequence using the ground-truth, but excluding the first 10 frames of each sequence. The SSIM results can be found in the supplementary material, together with additional qualitative comparisons of the methods.

Compared methods. To the best of our knowledge the only blind video denoising method from the literature is the F2F algorithm [23,21]. Besides comparing with F2F we also compare with a reference FastDVDnet network trained in a supervised setting specifically for each considered noise type and intensity. This will serve as a *gold standard*, and we will show that our MF2F results attain and sometimes surpass its performance. These supervised FastDVDnet networks are retrained as the original FastDVDnet [60] except for Gaussian noise for which we used the weights provided by the authors. We also include the result of VBM3D [17] in which the noise parameter is set to yield the best result. In the comparison we also include the performance of the weak video denoiser used as teacher network. The teacher network is the FastDVDnet for Gaussian noise for which eight noise parameters $\{\sigma_i\}_{i=1}^8$ are fine-tuned. The spatial noise map is obtained by splitting the image range in eight segments, and assigning each pixel to a segment based on its value. Each segment has a corresponding σ_i . This allows to roughly handle signal dependent noise.

Online video denoising. The quantitative results of the online MF2F algorithm are reported in Table 1. We can see that for Gaussian noise the results of MF2F exceed the performance of the supervised FastDVDnet network trained specifically on that noise level. For Poisson and correlated noise the performance is very close to the supervised FastDVDnet specifically trained for each type and level of noise. In all experiments we observe a PSNR increase of about 3dB with respect to F2F. This corresponds to a noise reduction by a factor 2, which is expected from a network that exploits the redundancy of 5 frames compared against a single frame method. We also observed reconstruction artifacts in the

³ <https://media.xiph.org/video/derf>

⁴ <http://www.vision.ee.ethz.ch/ntire20/>

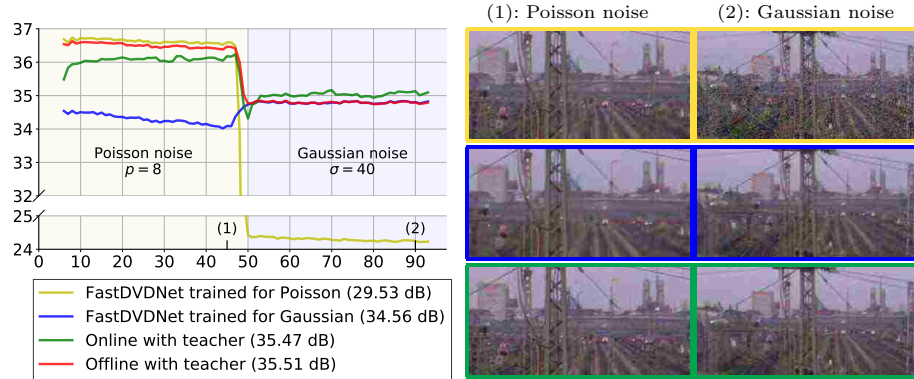


Fig. 4: Adaptation to changes in the noise properties. We simulate a sequence with Poisson noise for the first half and Gaussian noise for the second half. The frames (1) and (2) corresponds to Poisson and Gaussian noise respectively. Pretrained method for the specific noise types perform poorly on the other half (yellow and blue), where the propose methods (online and offline) are able to cope with the abrupt change.

F2F results that might be due to the poorer occlusion mask used, compared to ours.

From Table 1 we can see that fine-tuning using a teacher network has a positive impact on the results in terms of PSNR. In the case of box noise the teacher network leads to a slightly lower PSNR. The reason is that the teacher was not trained for correlated noise. Even so, the use of the teacher network improves the denoising of regions with fast motion, as can be seen in Fig. 3.

The online fine-tuning of the network permits to quickly adapt to changes in the noise properties. The PSNR plot in Fig. 4 shows the per-frame PSNR computed on a sequence in which the noise switches from Poisson ($p = 8$) to Gaussian ($\sigma = 40$) at frame 50. While the two pretrained FastDVDnet networks performs well for their respective noise types, their performance strongly degrades for the other type. This failure is visible on the crop of Fig. 4 where the two first rows shows results from the FastDVDnet networks trained for Poisson and Gaussian, respectively. We observed that the network trained for Poisson performs poorly on the Gaussian noise (residual noise), whereas the network trained for Gaussian performs poorly on Poisson noise (oversmoothing). On the other hand, our proposed approaches are able to cope with the abrupt change of noise, and the online version even outperforms the network trained for Gaussian on the Gaussian section. The bottom row shows that the online method with teacher is able to restore fine details on both noise types.

Offline video denoising. The offline fine-tuning permits to adapt to the noise of a particular sequence. The results in Table 1 show that the performance of the offline methods is slightly superior to the online one. Moreover, often the PSNR



Fig. 5: Comparison of denoising results for Poisson noise ($p = 8$, top row) and demoisaicked Poisson noise ($p = 4$, bottom row). From left to right: noisy frame, F2F, offline without teacher, offline with teacher, supervised training.

Table 2: PSNR results for different training stacks

Stack at inference	Train with blind-spot at			Train with dilated	FastDVDnet
	$r = 3$	$r = 2$	$r = 1$	Stack $r = 1$	Supervised
Natural stack	29.678	31.737	35.527	35.613	35.071
Same as training	29.678	31.701	35.450	35.243	35.071

results without teacher are better. The difference lies in the way the fine-tuning is being performed. While the online fine-tuning is performed one stack at a time to produce a single frame, the offline fine-tuning is performed on a batch of 20 stacks for each gradient descent step. In Figs. 1 and 5 we can compare the results of the offline method with FastDVDnet and F2F for the Poisson and Box noise types. Note that our blind denoising recovers fine details comparable to those obtained with the supervised FastDVDnet trained for these specific noise types. As shown in Fig. 4 where the noise changes throughout the sequence, the offline method is able to handle temporally varying noise by learning to denoise the two types of noise present in a video with the same network.

Input stack options. Table 2 summarizes the results for the different fine-tuning stacks. With the *dilated stack* $\mathcal{S}'_t = [f_{t-4}, f_{t-2}, f_t, f_{t+2}, f_{t+4}]$ we use the frame f_{t-1} as target. We also considered “blind-spot” stacks by taking the target frame as positions $r \in \pm\{1, 2, 3\}$ and removing that frame from the natural stack, e.g. for $r = -2$ (i.e. $[f_{t-3}, f_{t-1}, f_t, f_{t+1}, f_{t+2}]$). The best performance was obtained for $r = \pm 1$. This is due to the degradation of the alignment as the target frame is separated from the current frame. The table also shows the results obtained using the same stack at inference time, or switching back to the natural. Best results are obtained when using the natural stack for inference.

Real videos. Fig. 6 shows results obtained on two sequences with unknown noise statistics. The first is extracted from footage of World War I⁵, in addition to the noise and the damaged parts of the film, there is also a strong compression that

⁵ <https://www.army.mil/>

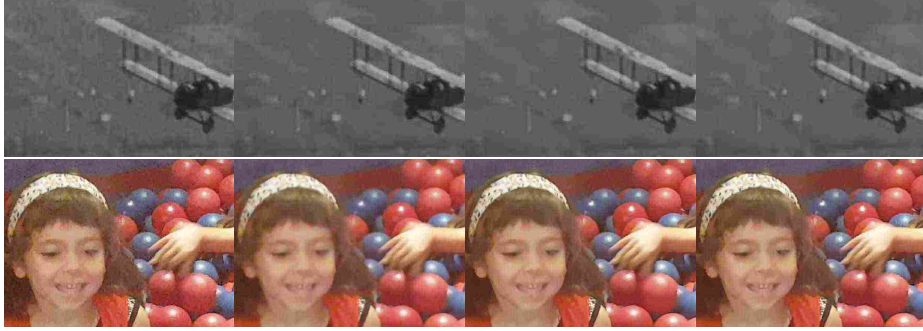


Fig. 6: Restoration of two real sequences. From left to right: original noisy video, F2F, offline MF2F, offline MF2F+T.

has been applied after digitalization. The second sequences is extracted from a video shot with a mobile phone (Samsung S7) in low light and processed by the camera pipeline and contains restoration artifacts. In both cases we observe that MF2F manages to remove the noise, while preserving more structure than F2F.

5 Conclusions

In this work we address the problem of blind video denoising. For that aim we extend to multi-frame denoising networks the self-supervised fine-tuning approach that was introduced in [22] but only for image denoising networks. The proposed approach demonstrates that by exploiting the temporal consistency in videos it is possible to train a network without ground truth and attain the performance of a network trained with supervision. A pre-trained network is fine-tuned by minimizing a loss that penalizes the error between the frame denoised by the network and the previous frame, after aligning them with an optical flow. In the regions where the alignment fails, we instead use the output of an additional weak denoiser (the *teacher*), which can also be fine-tuned. This prevents artifacts caused by the training bias that would otherwise result from the systematic alignment errors around motion discontinuities. The proposed approach demonstrates that by exploiting the temporal consistency in videos it is possible to fine-tune a video denoising network from only a few frames of a single noisy sequence and attain the performance of a network trained with supervision on a large dataset. This also allows to handle time-varying noise, which could be useful for vision systems exposed to varying conditions (for instance a surveillance camera at day and night).

This work opens interesting research perspectives. For instance, as in [61], *meta-learning* could be used to improve the adaptation speed of the pre-trained network, or the robustness of the teacher network. It would also be interesting to apply this approach to different domains where ground truth data is scarce (as in the case of medical imaging).

6 Acknowledgment

The authors gratefully acknowledge the support of NVIDIA Corporation with the donation of the Titan V GPU used for this research. Work partly financed by IDEX Paris-Saclay IDI 2016, ANR-11-IDEX-0003-02, Office of Naval research grant N00014-17-1-2552, DGA Astrid project "filmer la Terre" no ANR-17-ASTR-0013-01, MENRT. This work was performed using HPC resources from the Msocentre computing center of CentraleSuplec and cole Normale Suprieure Paris-Saclay supported by CNRS and Rgion le-de-France.

References

1. Abdelhamed, A., Lin, S., Brown, M.S.: A high-quality denoising dataset for smart-phone cameras. In: The IEEE Conference on Computer Vision and Pattern Recognition (CVPR) (June 2018)
2. Arias, P., Facciolo, G., Morel, J.M.: A comparison of patch-based models in video denoising. In: IVMSIP. IEEE (2018)
3. Assaf Shocher, Nadav Cohen, M.I.: "zero-shot" super-resolution using deep internal learning. In: The IEEE Conference on Computer Vision and Pattern Recognition (CVPR) (June 2018)
4. Batson, J., Royer, L.: Noise2Self: Blind denoising by self-supervision. In: Chaudhuri, K., Salakhutdinov, R. (eds.) Proceedings of the 36th International Conference on Machine Learning. Proceedings of Machine Learning Research, vol. 97, pp. 524–533. PMLR, Long Beach, California, USA (09–15 Jun 2019), <http://proceedings.mlr.press/v97/batson19a.html>
5. Boulanger, J., Kervrann, C., Bouthemy, P., Elbau, P., Sibarita, J.B., Salamero, J.: Patch-based nonlocal functional for denoising fluorescence microscopy image sequences. IEEE transactions on medical imaging **29**(2), 442–454 (2009)
6. Brooks, T., Mildenhall, B., Xue, T., Chen, J., Sharlet, D., Barron, J.T.: Unprocessing images for learned raw denoising. In: Proceedings of the IEEE Conference on Computer Vision and Pattern Recognition. pp. 11036–11045 (2019)
7. Brummer, B., De Vleeschouwer, C.: Natural image noise dataset. In: The IEEE Conference on Computer Vision and Pattern Recognition (CVPR) Workshops (June 2019)
8. Burger, M., Lucka, F.: Maximum a posteriori estimates in linear inverse problems with log-concave priors are proper bayes estimators. Inverse Problems **30**(11), 114004 (oct 2014). <https://doi.org/10.1088/0266-5611/30/11/114004>
9. Caelles, S., Maninis, K.K., Pont-Tuset, J., Leal-Taixé, L., Cremers, D., Van Gool, L.: One-shot video object segmentation. In: Proceedings of the IEEE conference on computer vision and pattern recognition. pp. 221–230 (2017)
10. Chang, Y., Yan, L., Chen, M., Fang, H., Zhong, S.: Two-stage convolutional neural network for medical noise removal via image decomposition. IEEE Transactions on Instrumentation and Measurement pp. 1–1 (2019). <https://doi.org/10.1109/TIM.2019.2925881>
11. Chen, C., Chen, Q., Do, M.N., Koltun, V.: Seeing motion in the dark. In: The IEEE International Conference on Computer Vision (ICCV) (October 2019)
12. Chen, C., Chen, Q., Xu, J., Koltun, V.: Learning to see in the dark. In: The IEEE Conference on Computer Vision and Pattern Recognition (CVPR) (June 2018)
13. Chen, J., Chen, J., Chao, H., Yang, M.: Image blind denoising with generative adversarial network based noise modeling. In: 2018 IEEE/CVF Conference on Computer Vision and Pattern Recognition. pp. 3155–3164 (June 2018)
14. Chen, X., Song, L., Yang, X.: Deep rnns for video denoising. In: Applications of Digital Image Processing (2016)
15. Claus, M., van Gemert, J.: Videnn: Deep blind video denoising. In: IEEE CVPRW (2019)
16. Coupé, P., Hellier, P., Kervrann, C., Barillot, C.: Nonlocal means-based speckle filtering for ultrasound images. IEEE transactions on image processing **18**(10), 2221–2229 (2009)
17. Dabov, K., Foi, A., Egiazarian, K.: Video denoising by sparse 3D transform-domain collaborative filtering. In: EUSIPCO (2007)

18. Davy, A., Ehret, T., Facciolo, G., Morel, J., Arias, P.: Non-local video denoising by CNN. CoRR **abs/1811.12758** (2018), <http://arxiv.org/abs/1811.12758>
19. Deledalle, C.A., Tupin, F., Denis, L.: Poisson nl means: Unsupervised non local means for poisson noise. In: 2010 IEEE international conference on image processing. pp. 801–804. IEEE (2010)
20. Dwibedi, D., Aytar, Y., Tompson, J., Sermanet, P., Zisserman, A.: Temporal cycle-consistency learning. In: The IEEE Conference on Computer Vision and Pattern Recognition (CVPR) (June 2019)
21. Ehret, T., Davy, A., Arias, P., Facciolo, G.: Joint demosaicing and denoising by overfitting of bursts of raw images. In: IEEE ICCV (2019)
22. Ehret, T., Davy, A., Morel, J.M., Facciolo, G., Arias, P.: Model-blind video denoising via frame-to-frame training. In: IEEE CVPR (2019)
23. Ehret, T., Davy, A., Morel, J.M., Facciolo, G., Arias, P.: Model-blind video denoising via frame-to-frame training. In: Proceedings of the IEEE Conference on Computer Vision and Pattern Recognition (CVPR) (June 2019)
24. Fernando, B., Bilen, H., Gavves, E., Gould, S.: Self-supervised video representation learning with odd-one-out networks. In: CVPR (2017), <http://arxiv.org/abs/1611.06646>
25. Gonzalez, M., Preciozzi, J., Muse, P., Almansa, A.: Joint denoising and decomposition using cnn regularization. In: The IEEE Conference on Computer Vision and Pattern Recognition (CVPR) Workshops (June 2018)
26. Gribonval, R., Nikolova, M.: On bayesian estimation and proximity operators (Jul 2018), <https://hal.inria.fr/hal-01835108>
27. Guo, S., Yan, Z., Zhang, K., Zuo, W., Zhang, L.: Toward convolutional blind denoising of real photographs. arXiv preprint arXiv:1807.04686 (2018)
28. Ilg, E., Mayer, N., Saikia, T., Keuper, M., Dosovitskiy, A., Brox, T.: FlowNet 2.0: Evolution of optical flow estimation with deep networks. In: IEEE Conference on Computer Vision and Pattern Recognition (CVPR) (2017)
29. Kang, E., Min, J., Ye, J.C.: A deep convolutional neural network using directional wavelets for low-dose x-ray ct reconstruction. Medical physics **44**(10), e360–e375 (2017)
30. Kay, S.: Fundamentals of statistical processing, volume i: Estimation theory: Estimation theory v. 1 (1993)
31. Kiku, D., Monno, Y., Tanaka, M., Okutomi, M.: Minimized-Laplacian residual interpolation for color image demosaicking. In: Sampat, N., Tezaur, R., Battiato, S., Fowler, B.A. (eds.) Digital Photography X. vol. 9023, pp. 197 – 204. International Society for Optics and Photonics, SPIE (2014). <https://doi.org/10.1117/12.2038425>, <https://doi.org/10.1117/12.2038425>
32. Kim, Y., Soh, J.W., Park, G.Y., Cho, N.I.: Transfer learning from synthetic to real-noise denoising with adaptive instance normalization (2020), <https://arxiv.org/abs/2002.11244>
33. Kirkpatrick, J., Pascanu, R., Rabinowitz, N., Veness, J., Desjardins, G., Rusu, A.A., Milan, K., Quan, J., Ramalho, T., Grabska-Barwinska, A., et al.: Overcoming catastrophic forgetting in neural networks. Proceedings of the national academy of sciences **114**(13), 3521–3526 (2017)
34. Krull, A., Buchholz, T., Jug, F.: Noise2void - learning denoising from single noisy images. CoRR **abs/1811.10980** (2018), <http://arxiv.org/abs/1811.10980>
35. Krull, A., Buchholz, T.O., Jug, F.: Noise2void - learning denoising from single noisy images. In: The IEEE Conference on Computer Vision and Pattern Recognition (CVPR) (June 2019)

36. Krull, A., Vicar, T., Jug, F.: Probabilistic noise2void: Unsupervised content-aware denoising. Tech. rep. (2019), <http://arxiv.org/abs/1906.00651>
37. Laine, S., Karras, T., Lehtinen, J., Aila, T.: High-quality self-supervised deep image denoising. In: Advances in Neural Information Processing Systems 32 (NeurIPS 2019) (2019)
38. Lebrun, M., Colom, M., Morel, J.M.: The noise clinic: a blind image denoising algorithm. *Image Processing On Line* **5**, 1–54 (2015)
39. Lehtinen, J., Munkberg, J., Hasselgren, J., Laine, S., Karras, T., Aittala, M., Aila, T.: Noise2noise: Learning image restoration without clean data. arXiv preprint arXiv:1803.04189 (2018)
40. Lempitsky, V., Vedaldi, A., Ulyanov, D.: Deep image prior. In: 2018 IEEE/CVF Conference on Computer Vision and Pattern Recognition. pp. 9446–9454 (June 2018). <https://doi.org/10.1109/CVPR.2018.00984>
41. Liu, C., Freeman, W.T.: A high-quality video denoising algorithm based on reliable motion estimation. In: ECCV. pp. 706–719 (2010)
42. Liu, D., Wen, B., Fan, Y., Loy, C.C., Huang, T.S.: Non-local recurrent network for image restoration. In: NIPS (2018)
43. Maggioni, M., Sánchez-Monge, E., Foi, A.: Joint removal of random and fixed-pattern noise through spatiotemporal video filtering. *Transactions on Image Processing* **23**(10), 4282–4296 (2014)
44. Marin, T., Srinivasan, V., Gl, S., Hellge, C., Samek, W.: Multi-kernel prediction networks for denoising of burst images. In: 2019 IEEE International Conference on Image Processing (ICIP). pp. 2404–2408 (Sep 2019). <https://doi.org/10.1109/ICIP.2019.8803335>
45. Metzler, C.A., Mousavi, A., Heckel, R., Baraniuk, R.G.: Unsupervised learning with stein’s unbiased risk estimator (2018), <http://arxiv.org/abs/1805.10531>
46. Mildenhall, B., Barron, J.T., Chen, J., Sharlet, D., Ng, R., Carroll, R.: Burst denoising with kernel prediction networks. In: IEEE Conference on Computer Vision and Pattern Recognition (CVPR) (2018)
47. Misra, I., Zitnick, C.L., Hebert, M.: Shuffle and learn: Unsupervised learning using temporal order verification. In: European Conference on Computer Vision. pp. 527–544 (2016)
48. Nam, S., Hwang, Y., Matsushita, Y., Joo Kim, S.: A holistic approach to cross-channel image noise modeling and its application to image denoising. In: The IEEE Conference on Computer Vision and Pattern Recognition (CVPR) (June 2016)
49. Plotz, T., Roth, S.: Benchmarking denoising algorithms with real photographs. In: Proceedings of the IEEE Conference on Computer Vision and Pattern Recognition. pp. 1586–1595 (2017)
50. Plötz, T., Roth, S.: Neural nearest neighbors networks. In: NIPS (2018)
51. Raphan, M., Simoncelli, E.P.: Learning to be bayesian without supervision. In: Schölkopf, B., Platt, J.C., Hoffman, T. (eds.) Advances in Neural Information Processing Systems 19, pp. 1145–1152. MIT Press (2007)
52. Ren, Z., Yan, J., Ni, B., Liu, B., Yang, X., Zha, H.: Unsupervised deep learning for optical flow estimation. In: Thirty-First AAAI Conference on Artificial Intelligence (2017)
53. Ronneberger, O., Fischer, P., Brox, T.: U-Net: Convolutional Networks for Biomedical Image Segmentation. *Miccai* pp. 234–241 (2015). https://doi.org/10.1007/978-3-319-24574-4_28
54. Salmon, J., Harmany, Z., Deledalle, C.A., Willett, R.: Poisson noise reduction with non-local pca. *Journal of mathematical imaging and vision* **48**(2), 279–294 (2014)

55. Sánchez Pérez, J., Meinhardt-Llopis, E., Facciolo, G.: Tv-l1 optical flow estimation. *Image Processing On Line* **2013**, 137–150 (2013)
56. Santhanam, V., Morariu, V.I., Davis, L.S.: Generalized deep image to image regression. *CoRR* **abs/1612.03268** (2016), <http://arxiv.org/abs/1612.03268>
57. Sermanet, P., Lynch, C., Chebotar, Y., Hsu, J., Jang, E., Schaal, S., Levine, S., Brain, G.: Time-contrastive networks: Self-supervised learning from video. In: 2018 IEEE International Conference on Robotics and Automation (ICRA). pp. 1134–1141. IEEE (2018)
58. Soltanayev, S., Chun, S.Y.: Training deep learning based denoisers without ground truth data. In: Bengio, S., Wallach, H., Larochelle, H., Grauman, K., Cesa-Bianchi, N., Garnett, R. (eds.) *Advances in Neural Information Processing Systems* 31, pp. 3257–3267. Curran Associates, Inc. (2018), <http://papers.nips.cc/paper/7587-training-deep-learning-based-denoisers-without-ground-truth-data.pdf>
59. Stein, C.M.: Estimation of the mean of a multivariate normal distribution. *Ann. Statist.* **9**(6), 1135–1151 (11 1981). <https://doi.org/10.1214/aos/1176345632>, <https://doi.org/10.1214/aos/1176345632>
60. Tassano, M., Delon, J., Veit, T.: Fastdvdnet: Towards real-time video denoising without explicit motion estimation. vol. *abs/1907.01361v1* (2019), <http://arxiv.org/abs/1907.01361>
61. Tonioni, A., Rahnema, O., Joy, T., Di Stefano, L., Thalaiyasingam, A., Torr, P.: Learning to adapt for stereo. In: *The IEEE Conference on Computer Vision and Pattern Recognition (CVPR)* (June 2019)
62. Tonioni, A., Tosi, F., Poggi, M., Mattoccia, S., Di Stefano, L.: Real-time self-adaptive deep stereo. In: *The IEEE Conference on Computer Vision and Pattern Recognition (CVPR)* (June 2019)
63. Vincent, P., Larochelle, H., Lajoie, I., Bengio, Y., Manzagol, P.A.: Stacked denoising autoencoders: Learning useful representations in a deep network with a local denoising criterion. *J. Mach. Learn. Res.* **11**, 3371–3408 (Dec 2010), <http://dl.acm.org/citation.cfm?id=1756006.1953039>
64. Vondrick, C., Shrivastava, A., Fathi, A., Guadarrama, S., Murphy, K.: Tracking emerges by colorizing videos. In: *The European Conference on Computer Vision (ECCV)* (September 2018)
65. Wang, N., Song, Y., Ma, C., Zhou, W., Liu, W., Li, H.: Unsupervised deep tracking. In: *Proceedings of the IEEE Conference on Computer Vision and Pattern Recognition*. pp. 1308–1317 (2019)
66. Wang, P., Zhang, H., Patel, V.M.: Sar image despeckling using a convolutional neural network. *IEEE Signal Processing Letters* **24**(12), 1763–1767 (2017)
67. Wei, D., Lim, J.J., Zisserman, A., Freeman, W.T.: Learning and using the arrow of time. In: *Proceedings of the IEEE Conference on Computer Vision and Pattern Recognition*. pp. 8052–8060 (2018)
68. Xue, T., Chen, B., Wu, J., Wei, D., Freeman, W.T.: Video enhancement with task-oriented flow. *IJCV* **127**(8), 1106–1125 (Aug 2019). <https://doi.org/10.1007/s11263-018-01144-2>, <https://doi.org/10.1007/s11263-018-01144-2>
69. Zach, C., Pock, T., Bischof, H.: A duality based approach for realtime tv-l 1 optical flow. In: *Joint Pattern Recognition Symposium*. Springer (2007)
70. Zhang, H., Mai, L., Xu, N., Wang, Z., Collomosse, J., Jin, H.: An internal learning approach to video inpainting. In: *The IEEE International Conference on Computer Vision (ICCV)* (October 2019)

71. Zhang, K., Zuo, W., Chen, Y., Meng, D., Zhang, L.: Beyond a Gaussian Denoiser: Residual Learning of Deep CNN for Image Denoising. *IEEE Transactions on Image Processing* **26**(7), 3142–3155 (7 2017). <https://doi.org/10.1109/TIP.2017.2662206>, <http://arxiv.org/abs/1608.03981><http://ieeexplore.ieee.org/document/7839189/>
72. Zhao, W., Deledalle, C.A., Denis, L., Maître, H., Nicolas, J.M., Tupin, F.: Ratio-based multitemporal sar images denoising: Rabasar. *IEEE Transactions on Geoscience and Remote Sensing* **57**(6), 3552–3565 (2019)
73. Zhong, Y., Li, H., Dai, Y.: Open-world stereo video matching with deep rnn. In: *The European Conference on Computer Vision (ECCV)* (September 2018)